Report - code automation for DSP algorithms implemented in bio-radar signals

Carolina Gouveia

10^{th} April 2020

1 Introduction

In this report, an automatic implementation of the Digital Signal Processing (DSP) algorithm for vital signs extraction is described in detail. Due to the Continuous Wave (CW) operation mode, bio-radar signals need to be carefully handled in order to extract correctly the respiratory waveform and its rate. Until now, algorithms were implemented manually and the complex signals were adjusted after visual inspection. However, an automatic implementation is required for real-time applications and also to ease the signal' inspection, saving time and resources.

In this sense, an automatic algorithm was developed using the previously established DSP algorithm as a basis. After its development, the algorithm was tested using a total of 66 signals, with different duration and characteristics. In order to test its efficiency, the rate of each signal was determined manually and compared with the one estimated by the algorithm. An accuracy error was also computed and it was possible to extract the correct breathing rate with an error inferior to ± 0.07 Hz.

This report is divided as the following: first the algorithm basis is reminded and the challenges of its implementation are identified, in Section 2. Then Section 3 presents the automatic algorithm flowchart and describes it in detail. The algorithm was tested in 66 different signals, that were acquired in different experiments and conditions. Results are presented in Section 4. Section 5 identifies some improvements that need to be done. Finally, conclusions and future work are going to be presented in Section 6.

2 Vital signs extraction algorithm

The bio-radar system is composed by a CW radar, which transmits a $f_0 = 10$ kHz sinusoidal signal with a carrier frequency equal to $f_c = 5.8$ GHz, towards to the target (the subject's chest-wall). The RF front-end receives the reflected signal, which is phase modulated due to the chest-wall displacement while the subject breathes.

The algorithm implemented to extract vital signs, namely the respiratory signal, is summarized by the block diagram in Fig. 1. The RF front-end is a homodyne transceiver and returns the signal already in baseband by performing an IQ down-conversion. However, since we are transmitting a sinusoidal signal with $f_0 = 10$ kHz, we are using a heterodyne front-end in practice. Therefore, the first step of this algorithm is to remove the f_0 component, by multiplying the received complex signal by its conjugate, resulting in signal $g(n)$. The

transceiver operates at a sampling rate of $f_s = 100$ kHz, so the next step is to decimate the $g(n)$ signal by an D factor equal to 1000. Hence, signal $d(n)$ has a new sampling rate equal to $f_d = 100$ Hz.

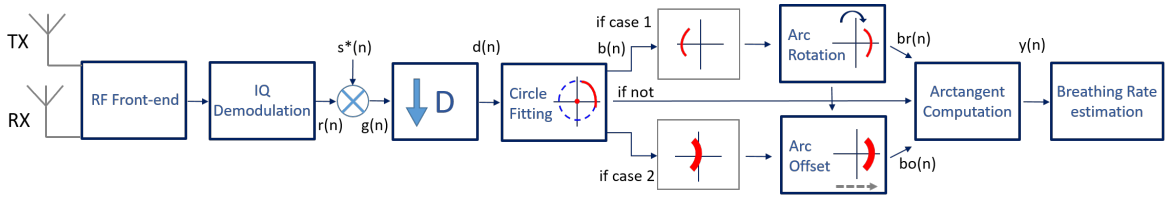

Figura 1: Basic DSP algorithm for vital signs extraction

The phase modulation of the received signal is perceived by an arc projection in the complex plane. Thus, the respiratory signal could be simply obtained by computing the arctangent of the $d(n)$ signal and the respiratory rate could be estimated after the arctangent computation. However this signal is not always centered in the complex plane origin and it can be, in fact, located in a random position. This happens because parasitic reflections are also received by the RF front-end, and these reflections occur in static objects adding a DC component to our signal. Therefore, it is necessary to track down the arc position and re-center it back to the origin. This can be performed by applying a circle fitting algorithm, that finds the circle that best fits the arc and estimates its center coordinates. These coordinates are then subtracted from the $d(n)$ signal, resulting in a $b(n)$ signal without a disruptive DC component.

Circle fitting is crucial for the algorithm efficiency. Some signals can be acquired in really harsh conditions resulting in non-perfect arcs, and turning it difficult for fitting algorithms to estimate the fitting circle correctly, along with its center coordinates. This could cause an incorrect re-center of the arc, making it cross the origin for instance. We will see later some possible outcomes of an unsuccessful circle fitting and how it can affect the breathing signal extraction.

After the DC component removal, a primary inspection of the signal's angle should be done in order to verify where the arc is located in the complex plane. If the arc is located between the second and the third quadrant, crossing the π value, wraps will occur on the extracted signal because the arctangent operation does not distinguish between π and $-\pi$ values. In this cases a rotation of the actual arc position is required resulting in signal $b_r(n)$.

As mentioned previously, sometimes the circle fitting is not performed successfully, leading to the arc to cross the origin. In this cases, wraps will also occur even if the arc is not centered between the second and third quadrants. Therefore, a small offset should be added, resulting in $b_o(n)$. Finally, the arctangent can be computed and the respiratory rate can be estimated from using the Welch method.

Until now the rotation and offset addition were performed manually, by inspecting each signal visually and performing customized rotations and offset insertions everytime it was needed. Real-time implementations require the execution of this task automatically, thus an automatic algorithm was developed considering all acquisition scenarios, with and without multipath or other issues related to the misalignment between the antenna beam and the radar cross-section of interest (that must be the subject's chest-wall and not the shoulders or neck, for instance).

3 Automatic algorithm implementation

3.1 Motivation

As we have seen previously, the main goal of the developed algorithm is to perform an arc correction automatically, avoiding any manual intervention. Since it is also required to determine the breathing rate automatically, the algorithm is programmed to re-locate the arc to what we consider an optimal position in the complex plane, but using the minimum iteration number in order to save computational resources. Fig.2 depicts an arc in an optimal position.

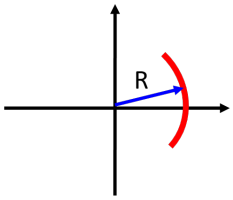

Figura 2: Arc located in an optimal position in the complex plane.

The optimal position is considered when the arc is centered between the first and the fourth quadrant, so its mean value is around 0°. There is also a small distance between the arc center and the complex plane origin, signed as R. This distance is important to perform correctly the phase demodulation and avoid sudden transitions or wraps, that could occur if the arc have samples crossing the origin. Although, it is important to note that this R distance is small enough, so its spectral cue near DC is not prominent. Finally, the interior concave part of the arc is faced to the origin. In this condition, the respiratory waveform is retrieved correctly and on its authentic shape.

In practice, the obtained arcs can assume different shapes and positions in the complex plane. Figures 3 to 5 show different examples of respiratory signals acquired in real case scenarios. These signals are already without the DC component, but are not corrected yet, so we can evaluate what happens if we do not correct them. Real case scenarios encompass issues such as multipath fading, constructive and destructive interference, parasitic reflections, misalignment between the antenna beam and the subject chest-wall or other motions of the subject that changes the mean value suddenly. All these issues affect the arc shape and hence hamper the successful recover of the original respiratory waveform and its rate estimation.

For instance, when the amplitude of the acquired signal is too low and there is not sufficient samples to perform a circle fitting correctly, the arc could end up above the origin without reserving the R distance. This effect is depicted in Fig. 3(a). In this case, if we recover the breathing signal, some spikes will appear due to the samples that are crossing the origin, as presented in Fig. 3(b). It is possible to correct this by adding a small offset in the real axis, pushing over the arc and establishing the R distance.

Another example is represented in Fig. 4(a), where the arc varies between the first and second quadrant, crossing also the π value. In this example, the arc is not located in the optimal position so the mean value is no longer 0°, and the samples that cross π value are perceived as wraps in the recovered signal, as depicted in Fig. 4(b). The occurrence of wraps in the middle of the observation window will cause a sudden change of the mean value, which will increase the mean value spectral component as depicted in Fig. 4(c). This issue can

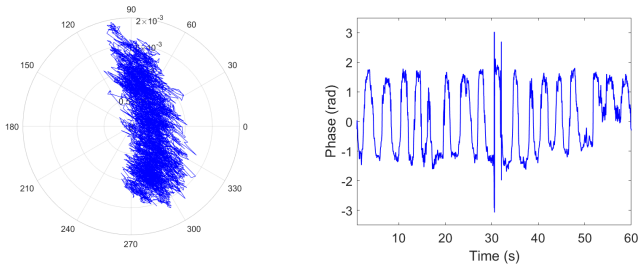

(a) (b)

Figura 3: Case 1: the arc is crossing the complex plane origin. (a) Arc located in the polar plot, (b) Breathing signal extraction

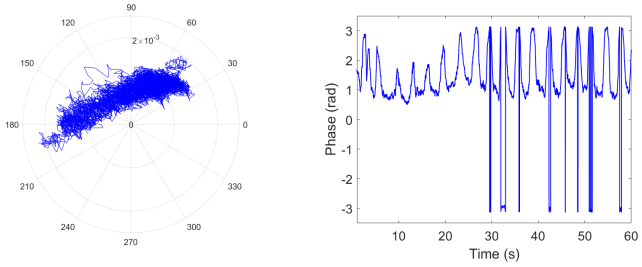

(a) (b)

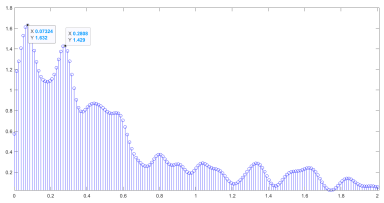

(c)

Figura 4: Case 2: the arc is located between the first and second quadrant. (a) Arc located in the polar plot, (b) Breathing signal extraction, (c) Frequency spectrum for this case.

be corrected by rotating the arc to the desired position. On the other hand, if the signal is completely centered in the π value (Fig.5), it might be possible to recover the spectral component correctly, but the waveform is completely distorted, as shown in Fig. 5(b). In this case, the arc should also be rotated to assure accurate results.

Finally, Fig. 6 shows the case when the arc is located in an optimal position and how its spectrum should look like.

3.2 Automatic algorithm implementation

The automatic implementation of the DSP algorithm represented by the block diagram in Fig. 1, can be achieved by following the flowchart depicted in Fig. 7. The algorithm is divided in three main stages that indicate how deeper it is required to go in the algorithm to correct the arc. Each stage is handled while certain conditions are verified.

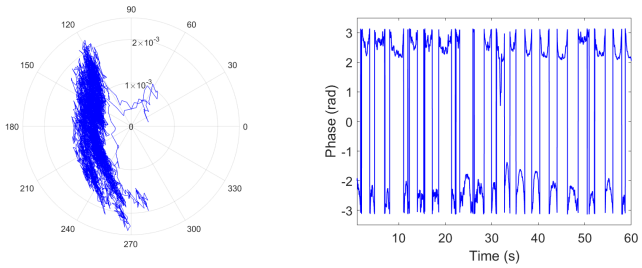

(a) (b)

Figura 5: Case 3: the arc is centered in the π value. (a) Arc located in the polar plot, (b) Breathing signal extraction

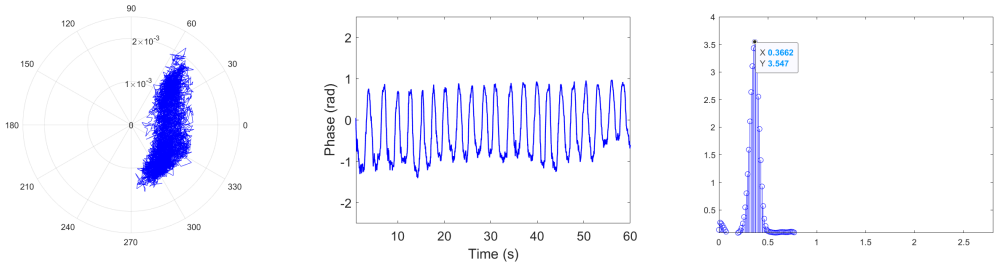

(a) (b) (c)

Figura 6: Case 4: the arc is located in the optimal position. (a) Arc located in the polar plot, (b) Breathing signal extraction, (c) Frequency spectrum for this case.

The algorithm starts by inspecting the arc position in the complex plane. If there is any sample of the arc between $\frac{-6\pi}{8}$ and $\frac{6\pi}{8}$, the first stage of the algorithm begins. The arc is rotated $\frac{\pi}{5}$ while that condition is verified (the condition is schematized in Fig. 8). However, it might happen that the stage 1 condition is always verified, if the arc is in the same situation as depicted in Fig.3. Due to these cases, the stage works according to a counter of rotations, in order to avoid an infinite loop. If this counter sums 10 turns, it means that the arc position performed a full 2π rotation, turning back to its initial position. In this case, we step forward in the algorithm and enter in the second stage.

The big majority of the tested signals were correctly recovered on the first stage. The threshold of $|\frac{6\pi}{8}|$ was selected rather than using $|\frac{\pi}{2}|$ directly, because there are some arcs that are large enough to pass the $|\frac{\pi}{2}|$ value in consecutive rotations.

If the algorithm arrives to the second stage, it means that it is on its original position, which is not the desired one. In this case, we could either rotate an uncertain number of times, that varies largely from case to case, or we can act on that signal directly, by firstly inspecting if it is parallel to the y axis (stage 2) and secondly by adding an offset until there are no negative real samples (stage 3).

Focusing firstly on the second stage, it starts by inspecting the arc shape and its position relatively to both real and imaginary axis. This inspection is made by computing the maximum and minimum values of both real and imaginary components, respectively, and then compute the width for each axis, as depicted in Fig. 9.

Furthermore, a polynomial fit is made in order to determine the arc orientation, as its

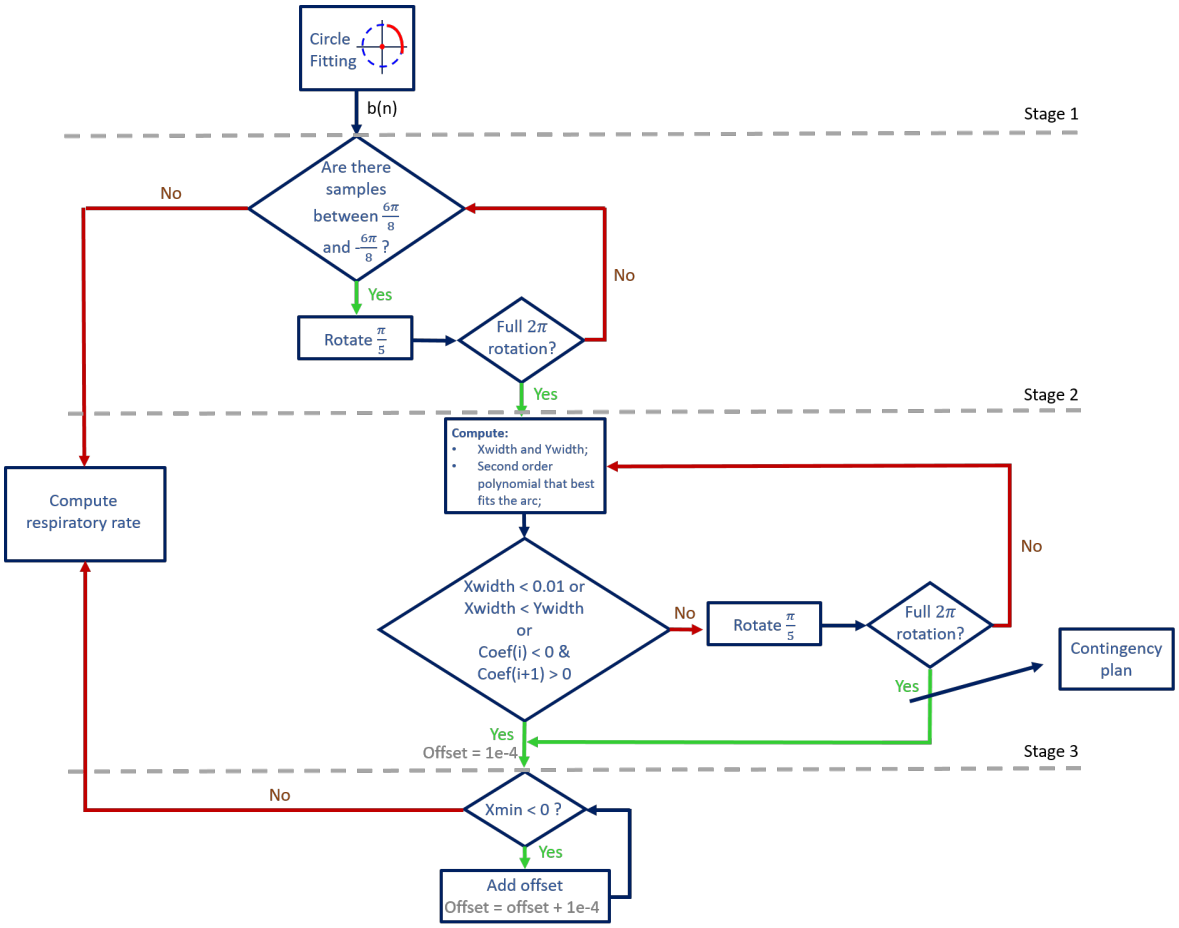

Figura 7: Automatic algorithm flowchart

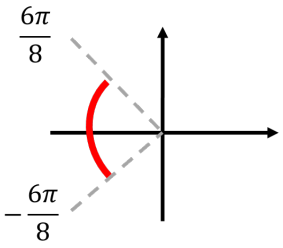

Figura 8: Schematics of the conditions that are ascertained on stage 1

interior part should be faced towards the origin. From this polynomial, the second order term ($Coef(1)$) is evaluated and a condition is settled according to its sign. In other words, the arc can be seen as a parabola, that has negative sign if it is turning downwards or positive sign if it is turning upwards (see Fig. 9). By visual inspection, it was defined that the arc is in the correct position on the transition from negative sign to positive sign. Thus, the arc is once again rotated $\frac{\pi}{5}$, while the following conditions are verified:

1. The *Xwidth* is higher than 0.01;

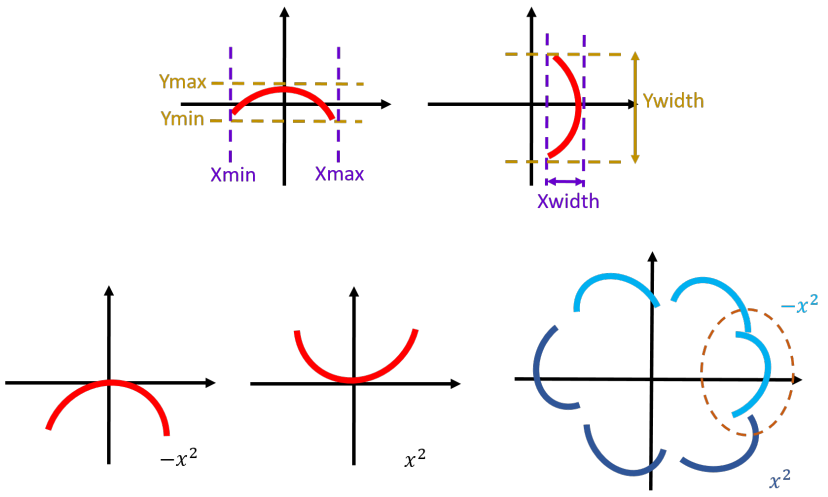

Figura 9: Schematics of the conditions that are ascertained on stage 2

2. The $Xwidth$ is higher than $Ywidth$;

3. The $Coef(1)$ is positive, or if it is negative, it is not positive on the next iteration.

In order to avoid infinite loops, a stop condition was settled similarly to the first stage, followed by a contingency plan. If a second counter sums 10 turns, a larger $Xwidth$ is allowed by changing the first condition to $Xwidth > 0.03$ and the counter returns to zero. The algorithm of stage 2 is then repeated considering this new condition, but this time the $Coef(1)$ is neglected. When the counter arrives to 10 turns for the second time, the algorithm enters in the Stage 3 independently on the arcs position.

The third stage simply adds an offset while the arc has samples with negative real part. It starts with a small offset (equal to $offset = 1e^{-4}$) and this offset is incremented in equal portions. The offset is only added in the real part of the complex signal.

At the end of the third stage, the signal is ready for the respiratory rate estimation.

3.3 Breathing rate estimation

The breathing rate estimation is performed by following the flowchart presented in Fig. 10. First, the arctangent of the complex signal is computed and its mean value is removed to avoid that the higher peak detected corresponds to DC, rather than the respiratory frequency. Then, the Welch method is implemented using Hamming windowing, with 50% of overlap. In order to ensure the correct peak detection an interpolation is made by a 10 factor. Then, a peak finder algorithm is applied and the detected peaks are sorted in descended order.

It is expected that the highest peak is from the respiratory component, but unfortunately this is not always verified. As we saw previously, a peak near DC can increase its magnitude if the mean value changes abruptly in the complex signal that is being inspected. This can happen when the subject moves randomly or changes its position during the monitoring period. In this case, the algorithm considers the second highest peak rather than the first one.

All in all, the Welch method presented better results when comparing with a simple FFT, and thus it was the selected method. However, it does fail when the respiratory frequency

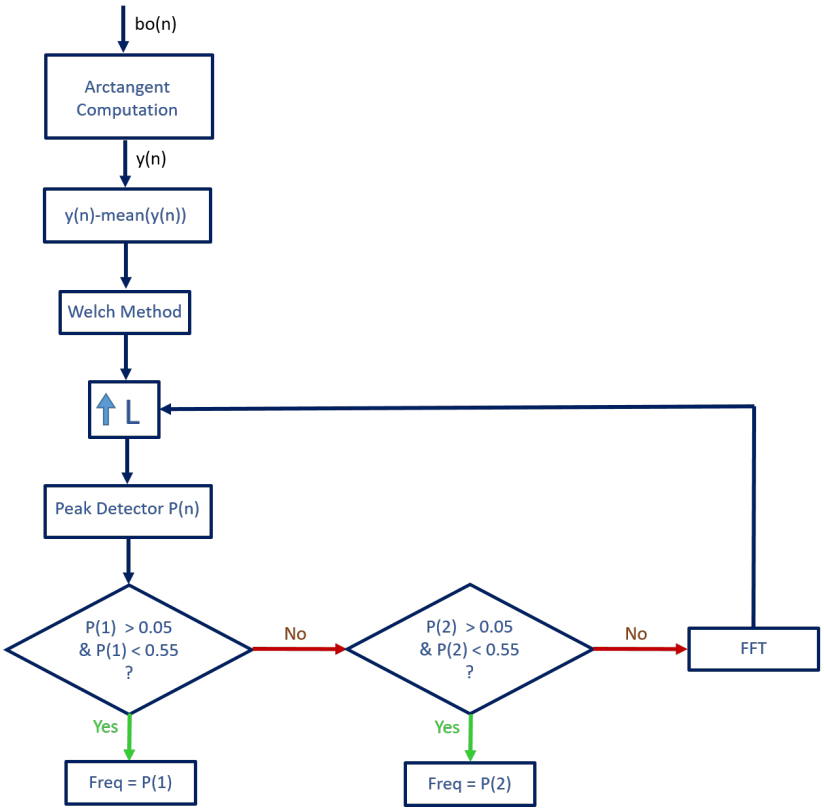

Figura 10: Breathing rate estimation algorithm flowchart

is too low. More specifically, if the breathing rate is around 0.1 Hz (6 breaths per minute), the Welch method does not have enough precision to distinguish that peak correctly. In that case, the FFT is performed in order to obtain an accurate estimation.

4 Results Discussion

In this section the automatic algorithm was implemented in 66 signals, which were acquired under different monitoring conditions. For each signal, the breathing rate was manually estimated and then compared with the rate detected by the automatic algorithm. For comparison purposes, the estimated breathing rate was achieved by counting the number of peaks per minute in one-minute signals and/or extrapolating the number of peaks of half-minute signals to one full minute.

Results are presented in tables 1 to 4, along with the absolute error, respectively. From the 66 signals, only 19 achieved Stage 2 (they are identified in tables with the pink color). From the remain, 27 were corrected in Stage 1 (identified in blue color) and 20 did not require any correction at all. Since most of the signals did not required heavy process (Stage 2), it is possible to conclude that stage 1 can not be skipped and should indeed be tried in first place, since it is sufficient for the arc correction in most cases. Anyway, if it is extremely necessary, the algorithm from Stage 2 and beyond can successfully determine the breathing rate accurately, as we will see further.

4.1 Chest-wall simulator signals

First of all, the algorithm was implemented in signals acquired in a controlled experiment. Instead of having a subject breathing, we used the Chest-Wall Simulator (CWS) to emulated the chest-wall motion that occur due to the cardiopulmonary function. The CWS is composed by a moving plate, that goes back and forward with the same frequency (in this case 0.4 Hz) and amplitude.

These signals served to evaluate the precision of the algorithm on determining the breathing rate accurately, since the 0.4 Hz frequency must be detected. The obtained results are disposed on table 1.

Tabela 1: Breathing rate results for CWS experiment

Signal Nº	**Measured Breathing Rate [Hz]**	**Nº of peaks (per 60 sec)**	**Estimated Breathing Rate [Hz]**	**Error [Hz]**
1	0.4	24	0.4	0.00
2	0.4	24	0.4	0.00
3	0.4	24	0.4	0.00
4	0.29	0	0	0.29
5	0.4	24	0.4	0.00

By analyzing the obtained results, it is possible to conclude that the automatic algorithm is efficient. The only case that failed was the one from signal 4, where the plate was not moving at all and hence the frequency of noise was extracted. This might be corrected by computing the variance of the signal during some time and establish a breathing rate equal to zero if the variance value is closed to zero.

4.2 Psylab signals

These signals were acquired in an experiment where the subjects were watching videos while being monitored. The radar located in front of the subject and each signal has 1 minute duration.

Table 2 present signals from 4 different subjects, identified by the capital letters of their first and last names. The conditions where this signals were captured are the most common in bio-radar applications, since the radar is in front of the subject and he/she was still during mostly of the time. However, there were some occasions where the subject had to move for some reason, turning the algorithm performance more challenging. In overall, it was possible to determine the breathing rate accurately, with a mean error equal to 0.0125.

4.3 Texboost signals

These signals were acquired using textile antennas located in the side lumber support of a car seat. The subject was seated, with the arms raised (emulating the driver position) and his/her breath was monitored. Signals presented in table 3 were not acquired with the same antennas, neither in the same exact position of the side lumber support. In fact, it was difficult to find a position that could detect the chest-wall motion with acceptable amplitude for all subjects, therefore these signals can test the limits of detection from the automatic algorithm.

Tabela 2: Breathing rate results for Psylab experiment

Signal Nº	Measured Breathing Rate [Hz]	Nº of peaks (per 60 sec)	Estimated Breathing Rate [Hz]	Error [Hz]
		Subject 1 - NB		
1	0.29	20	0.3333	0.04
2	0.34	21	0.35	0.01
3	0.37	23	0.3833	0.01
4	0.32	18	0.3	0.02
5	0.3	19	0.3167	0.02
6	0.3	18	0.3	0.00
		Subject 2 - AS		
1	0.30	18	0.3	0.00
2	0.26	15	0.25	0.01
3	0.27	17	0.2833	0.01
4	0.28	17	0.2833	0.00
5	0.26	15	0.25	0.01
6	0.27	16	0.2667	0.00
7	0.26	16	0.2667	0.01
		Subject 3 - LA		
1	0.29	17	0.2833	0.01
2	0.31	18	0.3	0.01
3	0.17	11	0.1833	0.01
4	0.21	14.5	0.2417	0.03
5	0.23	14	0.2333	0.00
6	0.28	16	0.2667	0.01
7	0.29	17	0.2833	0.01
8	0.29	18	0.3	0.01
		Subject 3 - ACM		
1	0.45	25	0.4167	0.03
2	0.35	22	0.3667	0.02
3	0.37	22	0.3667	0.00
4	0.37	22.5	0.3667	0.00
5	0.35	20	0.3333	0.02
6	0.31	18	0.3	0.01
7	0.35	20	0.3333	0.02
8	0.40	21.5	0.3583	0.04
9	0.35	20	0.3333	0.02
10	0.33	19	0.3167	0.01
11	0.36	21.5	0.3583	0.00

Due to the monitoring harsh conditions, there were some signals affected by multipath and low SNR. Some examples of these signals are depicted in Fig. 11 to Fig. 13.

For instance, Signal 14 with its polar diagram presented in Fig. 11 presents a normal arc shape which was corrected only using Stage 1. However, Signal 7 and Signal 10 in Fig. 13 and

Tabela 3: Breathing rate results for Texboost acquired signals

Signal Nº	**Measured Breathing Rate [Hz]**	**Nº of peaks (per 60 sec)**	**Estimated Breathing Rate [Hz]**	**Error [Hz]**
1	0.18	12	0.2	0.02
2	0.21	12	0.2	0.01
3	0.21	13	0.2167	0.01
4	0.18	10	0.1667	0.01
5	0.20	12	0.2	0.00
6	0.20	12	0.2	0.00
7	0.20	12	0.2	0.00
8	0.21	14	0.2333	0.02
9	0.19	12	0.2	0.01
10	0.24	16	0.2667	0.03
11	0.20	13	0.2167	0.02
12	0.16	10	0.1667	0.01
13	0.16	9	0.15	0.01
14	0.15	9	0.15	0.00

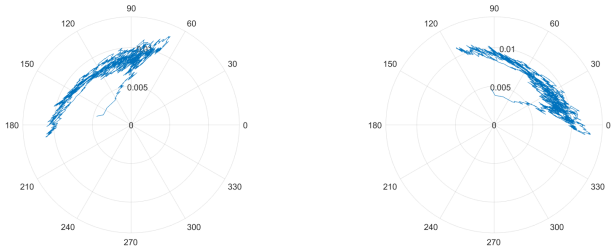

(a) (b)

Figura 11: Signal 14: (a) Before arc correction, (b) After arc correction.

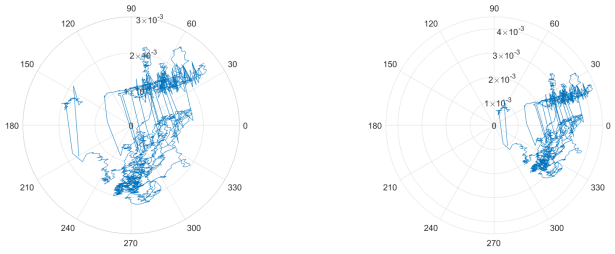

(a) (b)

Figura 12: Signal 7: (a) Before arc correction, (b) After arc correction.

Fig. 12 respectively, were too distorted and the Stage 2 and 3 were required. The Signal 14 case had an estimated rate of 9 breaths per minute which was determined by the algorithm successfully. On the other hand, Signal 7 could also determine its rate correctly and with the

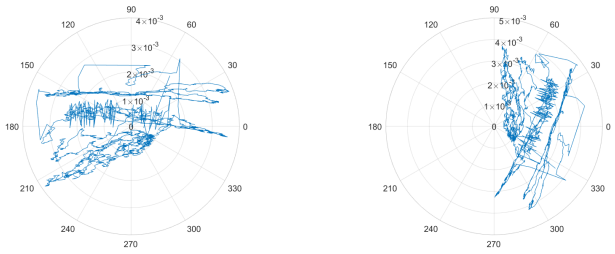

(a) (b)

Figura 13: Signal 10: (a) Before arc correction, (b) After arc correction.

same precision, despite being a noisy signal. The rate of Signal 10 was determined with an error of 0.03, which is also accepted.

4.3.1 Six volunteers experiment

The signals from this experiment were also acquired under the same circumstances as the ones presented in the previous section. However, they deserve a highlight since they were the ones used to draft the primary versions of the automatic algorithm. This group of signals have good SNR signals (for instance Signal 1 and Signal 2), really low frequency signals (Signal 3 and Signal 4) and signals with high changes of the mean value (Signal 9 and Signal 13). In all cases, it was possible to determine the breathing rate accurately.

Tabela 4: Breathing rate results for six volunteer experiment

Signal Nº	**Measured Breathing Rate [Hz]**	**Nº of peaks (per 60 sec)**	**Estimated Breathing Rate [Hz]**	**Error [Hz]**
1	0.22	12	0.2	0.02
2	0.21	13	0.2167	0.01
3	0.08	6	0.1	0.02
4	0.1	6	0.1	0.00
5	0.29	16	0.2667	0.02
6	0.21	12	0.2	0.01
7	0.33	20	0.3333	0.00
8	0.31	18	0.3	0.01
9	0.28	18	0.3	0.02
10	0.35	18	0.3	0.05
11	0.25	16	0.2667	0.02
12	0.22	12	0.2	0.02
13	0.16	14	0.2333	0.07
14	0.24	16	0.2667	0.03
15	0.32	19	0.3167	0.00

5 Challenges identification

Until now we have seen that the proposed automatic algorithm can recover successfully the breathing signal and compute its rate accurately, with a maximum error of 0.07 Hz. However, there are still some improvements that should be done.

- First, the computational effort should be reduced and the execution time decreased as maximum as possible, by search and deleting possible redundancies.
- The algorithm should encompass cases where there is no motion at all and thus identify 0 Hz.
- The boundary conditions should be verified on Stage 2 and Stage 3, by implementing this algorithm for more signals e identify where it could fail. The main goal is trying to define boundary conditions that suits all signals.
- The offset added in the third stage is too high sometimes and not necessary in all cases. High offset decrease the signal amplitude. In this conditions is still possible to estimate the respiratory accurately on the total number of tested signals. Even though, it is still possible to compromise other signals acquired in future. A solution that fits all cases, including arcs with disperse samples should be developed.

6 Conclusion

In this work, an automatic algorithm is presented to correct the arcs position in the complex plane after the DC component removal. This correction is required in order to extract correctly the respiratory signal and compute accurately its rate. The algorithm is composed by three main stages, where each one represents the necessary complexity of the signal processing, required to extract the desired signal successfully. The first stage only rotates the arc, so it varies between the first and fourth quadrant, avoiding wraps. The second stage is performed if the first fails, and the arc is rotated according to the arc shape. Finally, in third stage an offset in the real component is added, assuming that the arc is already in the correct position. This offset push the arc over from the complex plane origin. In the end, the breathing rate is estimated using the Welch method. However, a traditional FFT is performed if low rates are detected, because Welch method have not sufficient precision.

This algorithm was tested in 66 signals and the breathing rate was determined with low error. Furthermore, 40 % of the signals were corrected in the first stage and only 28 % required more complex process. These 66 signals encompassed several monitoring scenarios, with different antennas, and thus testing the limits of the algorithm.

Although, there are still space for improvements, by testing this algorithm in more signals and verifying the boundary conditions of the algorithm. Moreover, the third stage needs to be improved in order to avoid additional offset which could not required.